

Corona discharge in the steam for electrostatically enforced condensation

Michael Reznikov

Senior Member, IEEE
Physical Optics Corporation
1845 205th Street
Torrance, CA 90501, USA
mreznikov@poc.com

Phil Willems

Physical Optics Corporation
1845 205th Street
Torrance, CA 90501, USA
pwilkinson@poc.com

Abstract -- The corona discharge in the steam is investigated theoretically and experimentally in means of implementation with the steam condenser for the improved phase-change rate. The considered phenomena include the nucleation of water vapor on mobile charge carriers, the electrohydrodynamic vapor flow toward the condenser wall and the thermodynamics of the charged micro-droplet. The average size of micro-droplet is estimated in the dielectrophoretic model and compared with published experimental data of others. Experimental investigation of corona-supported condensation confirms the improvement in the condensation rate.

Index Terms—Corona, Dielectrophoresis, Thermal engineering

I. INTRODUCTION

The phase-change heat exchangers are widely used from miniature heat pipes in notebooks to steam condensers of power plants where the liquefying typically occurs due to the passive thermal exchange. The temperature on the condensing wall is lowered below the dew point and the depletion (due to the condensation) of vapor phase is constantly compensated by the diffusion. Because the mass flow rate (and the carried heat flux) depends on the gradient of vapor pressure, the high thermal flux is achieved by the intensive cooling of condenser that is the energy consuming (in the best case) or even impossible with the air convection cooling at summer time. In fact, the geothermal power plant's output drops to less than two-thirds of the rated capacity during the hotter portions of the year, primarily due to increased condenser pressure that decreases the heat extraction from the geothermal brine to lower the temperature. In general, the air-cooled condensers significantly contribute to the cost of generating electrical power, because of their size, associated capital cost (about 20% to 35% of the total plant cost), and the fan power consumed for the circulation of air. Therefore, any intensification of condensation potentially results in the additional generated power.

The presented work describes the concept of electrostatically enforced condensation, which is supported by the synergetic effect of a high-gradient electrical field and the vapor dielectrophoretic nucleation on charged droplets generated by corona discharge or electrospray. This innovative technology is developed on base of our previous works in the dielectrophoretic vapor enrichment [1-3].

II. THEORY

The concept of electrostatically enforced condensation (EEC) is based on the vapor dielectrophoretic nucleation on ions generated by the corona discharge or electrically charged droplets produced by the electrospray atomization. Due to the negative dielectrophoretic potential of the droplets, their evaporation is suppressed, which leads to depletion of the vapor phase compensated by diffusion. As a result, when charged nanodroplets are electrostatically transferred to the heat exchanger walls and discharged, the local vapor density near the wall exceeds the saturation level and condensation occurs at a higher temperature than it would occur at without electrostatic enforcement.

Water droplets are easily generated on ions [4] due to the native polarity of water molecules, which have a natural dipole moment, $\rho_o = 6.17 \times 10^{-28}$ C·cm. Any particle with a dipole moment, ρ_o , if placed in the gradient electric field of magnitude, E , experiences the dielectrophoretic force $F_{dp} = \rho_o \text{grad}E$, directed to the side of the increased field E . Polar water molecules drift in the gradient electric field and produce the gradient of vapor concentration. The stable state occurs when the drift and local diffusion flows are equal, which leads to the classic Maxwell distribution, $n = n_\infty \exp(U/kT)$, where the potential energy, U , of a molecule at distance, R , from the point charge, q , can be calculated by integration of dielectrophoretic force from distance R to infinity

$$U = \rho_o \int_R^\infty \text{grad}E dr = \rho_o q / (\epsilon_0 R^2). \quad (1)$$

Therefore, the gradient electric field induces the enrichment of water vapor, $\gamma I = pR/pv = \exp(U/kT)$ ($kT = 0.026$ eV), near the charged particle or very thin wire electrode. In practice, the corona current or even natural ionization of air produces ions that serve as centers for vapor condensation, thus producing droplets of water (fog).

If small droplets are not electrically charged, they easily evaporate, as demonstrated by Kelvin's equation for the saturated vapor pressure p^b near the surface of a drop with radius R

$$p^b = p_\infty \exp(2\sigma v^l / (N_A k T R)), \quad (2)$$

The work presents preliminary results of project supported by DOE grant DE-EE0005130.

where v^l is a molar volume in liquid (18 cm³ for water), N_A is Avogadro's number (6.02×10^{23}), p_∞ is the pressure of saturated water vapor above a flat surface, or 133 N/m² for water at 20°C, and $\sigma = 72.84 \times 10^{-3}$ N/m is the surface tension of water at room temperature. The vapor oversaturation (relative to the saturation pressure of vapor over the liquid flat surface) near the small droplet is illustrated in Fig. 1.

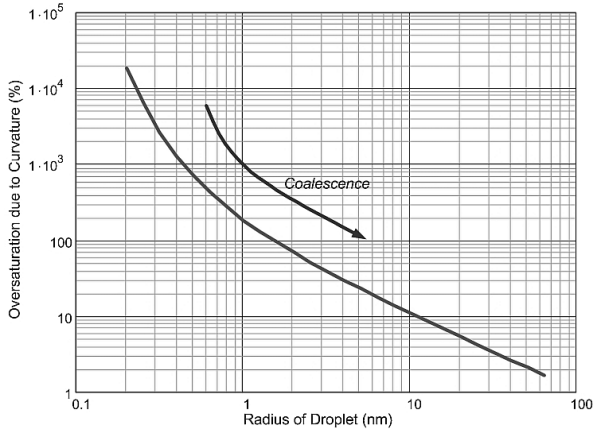


Fig. 1. Oversaturation of vapor near the water droplet relative to the saturated vapor pressure over the liquid flat surface

Fig. 1 shows that droplets of any size are not stable if proximity to the bulk water surface is close enough for the diffusion of vapor molecules. Nevertheless, in the absence of bulk water surface, droplets coalesce through the vapor phase – small droplets evaporate and locally increase the density of vapor, which leads to the growth of bigger droplets through condensation

Because of the dielectrophoretic potential of a charged droplet (see Fig. 2), the energy barrier for evaporation from such a droplet is increased, which may be interpreted as the decrement of effective surface tension (see Fig. 3) and, correspondingly, the saturated vapor pressure near the surface is lowered, as shown in Fig. 4.

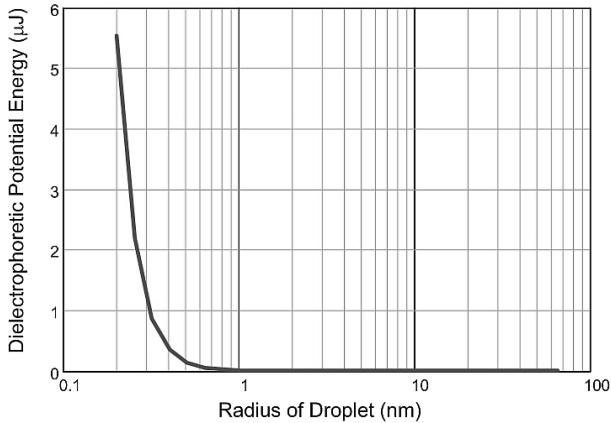


Fig. 2. Dielectrophoretic potential of the water molecule near the charged droplet

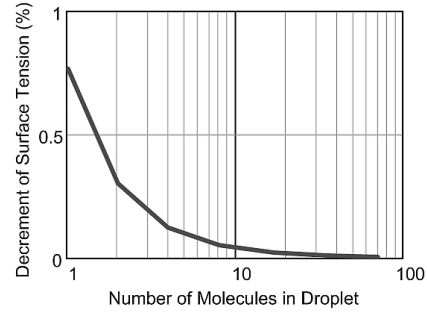


Fig. 3. Decrement of effective surface tension in the electrically charged droplet

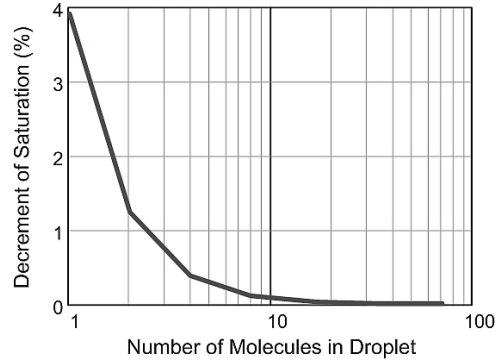


Fig. 4. Decrement of the vapor saturation pressure for the electrically charged droplet

A comparison of Fig. 3 and 4 illustrates that the electric charge significantly decreases the saturated vapor pressure relative to the neutral droplet of the same size. While the surface tension is decreased by less than 1 percent, the decrement of saturated vapor pressure varies in the range of a few percent. Of course, this does not change the instability of the droplet (i.e., the cluster of a few water molecules) relative to the bulk water. But the stability of nanodroplets increases in the vapor-droplets mixture, and droplets grow until equilibrium with the vapor phase is reached. If such a charged droplet reaches the boundary region with the flat liquid surface (for example, the surface of the condenser), the droplet begins to evaporate due to the lower vapor pressure in this region. But the drift of the droplet toward the water surface due to the electrostatic force leads to the direct deposit of the condensed phase to the bulk condensate. Therefore, the EEC process allows for highly localized condensation in the volume of vapor, with the subsequent acquisition of water clusters at the condenser surface.

While ions produced by corona carry the single charge, $e = 1.6 \cdot 10^{-19}$ C, the electrospray produces droplets with charge, q_R , at which the Rayleigh limit is exceeded and fission occurs

$$q_R = 8\pi\sqrt{\epsilon_0\gamma} \cdot r^3 \quad (3)$$

Eq. (3) shows that the total charge, q_R , carried by the droplet increases with the droplet radius, r , i.e. larger electrospray droplets bear charge, which significantly exceeds the single ion charge carried by droplets created due to the nucleation

of water vapors on ions in the humid air. This is illustrated in Fig. 5, which presents the results of the numeric calculation of the carried charge at varied radius of electro spray droplet that is based on Eq. (3).

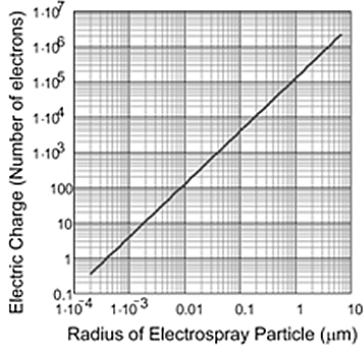


Fig. 5. Maximal electric charge carried by the electro spray droplet vs the radius of this droplet

The significant electric charge of electro spray droplets allows for the attraction of neutral (or single charge) aerosol. The polarizability of dielectric sphere, α , with dielectric permittivity, ϵ , is $\alpha = 3\epsilon_0 V_r (\epsilon - \epsilon_0) / (\epsilon + 2\epsilon_0)$, where $V_r = 4\pi r^3/3$ is the volume of sphere. The dielectrophoretic force, F_{dp} , acting on the aerosol droplet at the distance R from the center of droplet carrying charge, q , is

$$F_{dp} = \alpha \cdot E \cdot \text{grad}|E| = \frac{\alpha}{2} \text{grad}E^2 = \frac{2\alpha q^2}{\epsilon_0^2 R^5}. \quad (4)$$

Supposing the threshold value for dielectrophoretic potential, Φ_{dp} , is equal to kT , the equation for effective dielectrophoretic radius, i.e. radius of sphere, which limit the space around the electro spray droplet of radius, r , where all neutral particulate with radius, r_p , will be collected:

$$\Phi_{dp} = \int_R^{\infty} F(q_r, r_p) dx = kT. \quad (5)$$

The solution of Eq. (5) accounting for Eq. (4) and supposing the water-based aerosol, $\epsilon = 80\epsilon_0$ for R at varied radius of electro spray droplet, r , and radius of aerosol particle, r_p , is presented in Fig. 6.

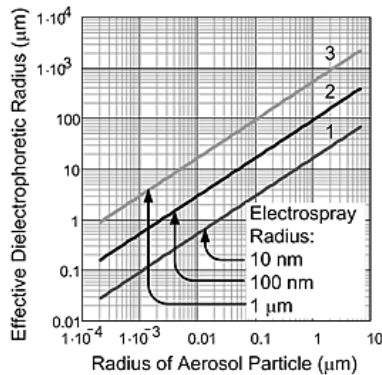


Fig. 6. The effective dielectrophoretic radius for capturing aerosol particles of

varied size calculated for radiuses of electro spray droplets (1) 10 nm, (2) 100 nm, and (3) 1000 nm.

It's not surprising that the bigger aerosol droplets collect the aerosol at the larger distance. Fig. 6 shows that the tenfold increase in the electro spray radius elevated the effective dielectrophoretic radius ~ 5 times.

III. PRELIMINARY EXPERIMENTS

To evaluate the effect of EEC of the steam, we assembled an experimental setup, which utilizes an electrically enforced condenser prototype that was previously built to demonstrate the electrostatic dehumidification of air in the ductless (closed circuit) clothes dryer. This setup is shown in Fig. 7.

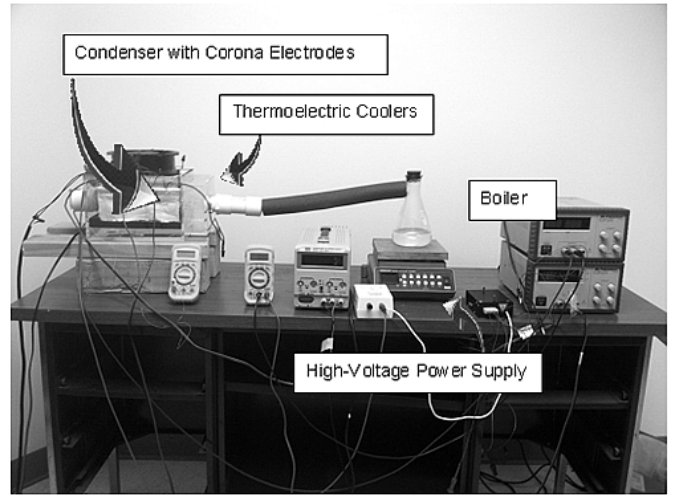


Fig. 7. First EEC experiment. The condenser (at left) is fed steam from the boiler (middle right).

The π -shaped aluminum condenser is contained within an acrylic chamber to ensure the containment of the steam while allowing the interior to be monitored. Acrylic was used in this initial test because the steam did not exceed a temperature of 100°C or the atmospheric pressure. The steam is directed from the boiler through the channel formed by the legs of the ' π ', where it condenses and is allowed to drip into a catch vessel. Atop the condenser are four thermoelectric, Peltier coolers (Ferrotec TEM 9501/242/160 B) to extract the heat released by the condensing steam into fan-cooled radiators. We used a thermocouple attached to the channel to judge the rate of condensation; higher condensation rates deposit more heat into the condenser and will raise its temperature.

An array of nine corona electrodes is installed within the condenser channel. In this experiment, all of the electrodes were energized to the same positive high voltage, producing a large electric field through which the steam passed on its way through the apparatus. The accumulation of charge on the condensate (distilled water is in fact a good electric isolator), leads to the discharge due to the dripping of

charged water into the condensate collector. Also, because corona electrodes in the narrow channel produced the notable electrohydrodynamic effect, the drag of charged droplets by the steam flow actually decreases the amount of water collected in the condenser. In order to eliminate the drag of the charged droplets, the exhaust of the condenser was sealed. This immediately resulted in an increase in frequency of the internal discharges. The results of the test are shown in Fig. 8.

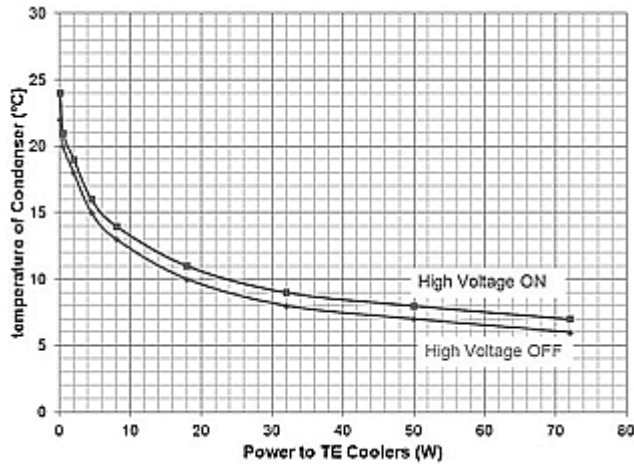


Fig. 8. Increment of temperature in the condenser at constant high voltage (8 kV) applied to corona wires and variable power applied to thermoelectric coolers

As Fig. 8 shows, the increment of temperature with high voltage applied is systematic, and the absolute difference in temperature increases with the power applied to the thermoelectric coolers. Fig. 9 presents the same data as the relative increment of the temperature.

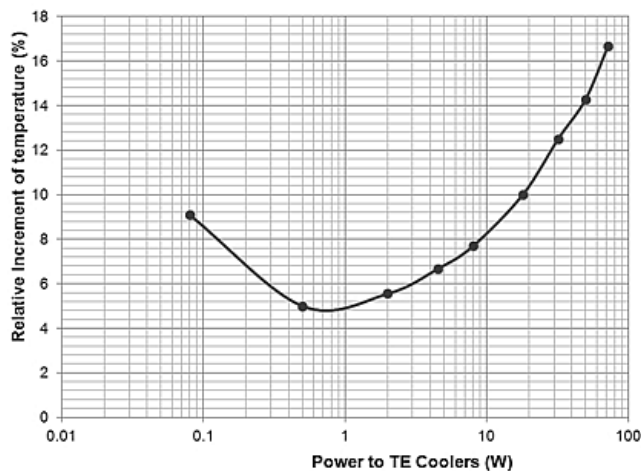


Fig. 9. Relative increment of temperature in the condenser at constant high voltage (8 kV) applied to corona wires and variable power applied to thermoelectric coolers.

Fig. 9 shows that the most efficient performance of ELSTEX is achieved at higher thermoelectric power. By

other words, the more efficient condensation requires not only the nucleation and delivery of vapor to the condensing wall, but also the ability of this wall to extract the latent heat. The increased efficiency of EEC at very low thermoelectric cooling power (practically negligible at the applied current of 250 mA, while the nominal current is 16 A) demonstrates the enforced heat exchange, with the practically passive exchanger, to the external heat sink.

Because the temperature in the condenser decreases with elevated thermoelectric power, the efficiency of EEC also varies: at low temperatures, condensation occurs efficiently enough without EEC while at overly high temperatures, the prototype did not create enough condensing power, and steam condensed outside of the prototype (which was investigated at low-power cooling).

IV. CONCLUSIONS

We developed a basic model of the electrostatically enforced condensation and demonstrated the feasibility of this approach by the preliminary conceptual test.

REFERENCES

- [1] M. Reznikov, "Dielectrophoretic Dehumidification of Gas Stream in Low and Moderate Electrical Fields," Electrostatics Society of America/IEEE, Joint Meeting, June 2003.
- [2] M. Reznikov, "Electrostatic Approach to Some Nontraditional Electrostatic Applications," Proceedings of the ESA/IEJ/IEEE-IAS/SFE Joint Conference on Electrostatics 2006, vol. 1, Laplacian Press, Morgan Hill, California, USA, p. 117, 2006.
- [3] M. Reznikov, A. Kolesov, R. Koziol, "Electrohydrodynamic Enforcement of Evaporation and Gas Flow," IEEE Industrial Applications Magazine, Vol. 47, No. 2, pp. 1036-1042, 2011.
- [4] M. Alonso, F.J. Alguacil, "Particle Size Distribution Modification During and After Electrical Charging: Comparison between a Corona Ionizer and a Radioactive Neutralizer," Aerosol and Air Quality Research, Vol. 8, No. 4, pp. 366-380, 2008..